Journal of Cell Science 106, 919-928 (1993)
Printed in Great Britain © The Company of Biologists Limited 1993

In vitro assembly properties of vimentin mutagenized at the β-site tail motif

Panos D. Kouklis[1,*], Mechthild Hatzfeld[2], Mariann Brunkener[1], Klaus Weber[2] and Spyros D. Georgatos[1,†]

[1]Programme of Cell Biology, European Molecular Biology Laboratory, 6900 Heidelberg, FRG
[2]Department of Biochemistry, Max Planck Institute for Biophysical Chemistry, 3400 Goettingen, FRG

*Present address: Department of Molecular Genetics & Cell Biology and Biochemistry & Molecular Biology, The University of Chicago, IL 60637, USA
†Author for correspondence

SUMMARY

The intermediate filament (IF) proteins vimentin, desmin and peripherin share a 9-residue sequence motif (β-site) located near the end of their COOH-terminal tail domain. Peptide inhibition experiments have previously suggested that the β-site is involved in interactions that limit the lateral growth of IFs and prevent inappropriate filament-filament associations. To investigate this question further, we have constructed and expressed, in *Escherichia coli*, hamster vimentin bearing different mutations in the β-site. We show here that a single exchange of glycine 450 with a valine residue, or an internal deletion of amino acids 444-452, strongly interferes with the normal assembly of IFs under in vitro conditions. These mutants polymerize into irregular fibrils that have a strong tendency to anastomose and laterally aggregate under isotonic conditions. In contrast, a non-conservative substitution of arginine 448 for glutamic acid does not significantly interfere with filament structure and yields subunits that polymerize into long, smooth filaments that show a slight aberration in thickness. All mutant proteins are soluble in low salt and form oligomers similar to the ones formed by wild-type vimentin. On the basis of these findings and on related observations, we propose that the tail domain of type III IF proteins contains important structural elements involved in lateral protofilament-protofilament interactions.

Key words: vimentin, β-site, tail domain, filament assembly

INTRODUCTION

One of the cardinal features of the intermediate filament (IF)-forming proteins is their tripartite substructure. These molecules possess a non-helical NH_2-terminal domain (head), a helical middle domain (rod), and a non-helical COOH-terminal domain (tail). The rod domain is involved in coiled-coil interactions and in other molecular associations mediating the formation of antiparallel, staggered tetramers (protofilaments) (for a recent review see Stewart, 1993). Further polymerization of IF proteins seems to involve complex interactions in which both the rod and the head domains play an important role (Albers and Fuchs, 1987, 1989; Herrmann et al., 1992; Hofmann and Herrmann, 1992; Kaufmann et al., 1985; Lu and Lane, 1990; Raats et al., 1990; Traub and Vorgias, 1983).

The contribution of the tail domain in IF assembly is currently being debated. On one hand, excision of the COOH-teminal region of cytokeratin and vimentin subunits does not interfere with filament formation in vitro (Hatzfeld and Weber, 1990; Wilson et al., 1992; Eckelt et al., 1992). On the other hand, tail-less glial fibrillary acidic protein (GFAP) does not assemble (Quinlan et al., 1989), while proteolytic digestion of a part of the tail domain in desmin (Kaufmann et al., 1985), vimentin (Shoeman et al., 1990) and neurofilament-L (Nakamura et al., 1993) seems to cause lateral aggregation of IFs and formation of thick bundles. Transfection studies show that an intact tail domain is required for normal desmin and neurofilament-M assembly in vivo (Raats et al., 1991; Wong and Cleveland, 1990). However, similar studies with tail-less cytokeratins have yielded conflicting results, suggesting that the tail domain may (Lu and Lane, 1990), or may not (Bader et al., 1991), be essential for IF assembly in living cells. Finally, recent experiments with tail-less vimentin (Eckelt et al., 1992) have shown that the mutant protein assembles into a variety of filamentous and non-filamentous structures in vivo.

In a previous study (Kouklis et al., 1991), we identified two sites (termed ε and β) that are conserved in the IF proteins vimentin, desmin and peripherin that interact with each other during in vitro polymerization. The ε site has been mapped between residues 364 and 416 in the vimentin rod, whereas the β-site has been localised between residues 444 and 452 in the vimentin tail. Assembly of vimentin subunits in the presence of a synthetic peptide imitation of the β-site, which presumably competes with the endogenous β-site, results in the formation of filaments that are much thicker than normal IFs. These and related observations (Birkenberger and Ip, 1990) have led us to propose that the tail domain (via the β-site) interacts with the rod domain (via the ε site), forming a 'loop' structure that ster-

ically prevents inappropriate lateral interactions between filaments or filament subunits.

To further investigate the role of the β-site in filament assembly, we have constructed recombinant vimentin forms mutated in this region. We show here that a single amino acid substitution at G-450, or an internal deletion comprising the entire β-site, severely interferes with protofilament-protofilament interactions and normal IF assembly in vitro. The structural implications of these results are discussed below.

MATERIALS AND METHODS

Construction of vimentin mutants and expression in *E. coli*

The cloning of wild-type hamster vimentin and its expression in *E. coli* have been described (Hatzfeld et al., 1992). To produce the vimentin tail mutants, wild-type vimentin containing the *Bam*HI and *Hin*dIII restriction sites was cloned into M13mp18 and single-stranded DNA was prepared from transformed CJ236 *E. coli* cells. Mutagenesis was carried out according to Kunkel et al. (1987), using the Bio-Rad mutagenesis kit (Bio-Rad, Richmond, CA). The oligonucleotides used for mutagenesis had the following sequences:

(1) ATTGATCACCTGTACATCCCTGGTTTC (G-450 to V);

(2) CACCTGTCCATCCTCGGTTTCCACTGT (R-448 to E); and

(3) AGAGGTTTCATTGATCACCTTAATCAGGAGTGTTCT (Δ 444-452).

Positive clones were selected after sequencing and cloned into the bacterial expression vector pINDU (Bujard et al., 1987). The plasmid DNA was then transformed into BL21 bacteria and the mutant sequence, as well as the sequence of the entire tail domain and of the conserved coil 2b motif of the deletion mutant (see Kouklis et al., 1992), was confirmed after the cloning procedure. To check for bacterial expression, cells from ~1 ml of culture were lysed in SDS sample buffer and samples were run on 10% SDS-gels (Laemmli, 1970).

Purification of vimentin from bacterial lysates

Bacterial cultures (300 ml) were grown at 37°C in LB containing 100 μg/ml ampicillin. The bacteria were harvested by low-speed centrifugation, resuspended in 150 mM NaCl, 10 mM Tris-HCl, pH 7.4, 1 mM PMSF, 2 μg/ml leupeptin, 2 μg/ml pepstatin, 2 μg/ml chymostatin, 2 μg/ml antipain and 2 μg/ml apronitin (lysis buffer) and lysed by sonication at 0°C. The lysates were spun at 12,000 ***g*** for 20 minutes and pellet was washed with lysis buffer containing 1% Triton X-100. After repelleting, the insoluble material was extracted once more with lysis buffer containing 1% Triton X-100 and 1 M urea. Finally, the insoluble residue was solubilized in 8 M urea, 10 mM Tris-HCl, pH 7.4, 1 mM EDTA, 1 mM DTT and the protease inhibitor cocktail described above (urea extraction buffer). The extract was clarified by centrifugation at 12,000 ***g*** for 35 minutes at 18°C and chromatographed in DEAE-cellulose using a 0-100 mM NaCl gradient (in the urea extraction buffer).

Cross-linking

For chemical cross-linking, we basically followed the procedure described by Geisler et al. (1992). The various vimentin forms (~400 μg/ml) were first dialysed from 8 M urea against 10 mM triethanolamine, pH 8.0, 1 mM β-mercaptoethanol (or against the same buffer plus 4 M urea) for 3 hours, at room temperature. To each 25 μl of sample 1.4 μl of 10 mg/ml EGS (ethylene glycol bis succinimidyl-succinate, dissolved in dimethyl sulfoxide) were added and the reaction mixtures were incubated at 37°C for 1 hour. At the end of this incubation, 1.4 μl of 1 M ethanolamine, pH 8.0, was added, followed by incubation at 37°C for 30 minutes and addition of 11 μl of 4× electrophoresis sample buffer. The reaction products were analysed by SDS-PAGE in 5% to 10% acrylamide gradient gels (Laemmli, 1970), and either silver-stained or probed with anti-vimentin antibodies.

Assembly of vimentin in vitro

Vimentin (typically 200 μg/ml, in urea buffer) was dialysed against isotonic buffer (150 mM KCl, 10 mM Tris-HCl, pH 7.4 and 1 mM DTT), or against low salt buffer (5 mM Tris-HCl, pH 7.4 and 1 mM DTT, for 3 hours at room temperature (~23°C). In a variation of this method, the vimentin was dialysed first against low salt buffer for 3 hours at 4°C, then against isotonic buffer for 18 hours at 4°C, and finally against isotonic buffer for 2 hours at 37°C. In the latter case all media contained 0.3 mM PMSF. Samples were applied to carbon-coated EM grids and negatively stained with 2% uranyl acetate. The specimens were examined in a Philips 400 or a Philips 301 electron microscope operated at 80 kV.

RESULTS

Expression and purification of vimentin tail mutants

To examine whether mutations in the region of the β-site would affect IF assembly, we constructed three different recombinant vimentin forms. Using site-directed mutagenesis, we changed G-450 to a V and R-448 to an E (Fig. 1). These two substitutions, and in particular the former, are expected to change the secondary structure of the tail domain in the neighborhood of the tetrapeptide TRDG (Fig. 1), a region with a relatively high potential for a β-turn. (The Chou and Fasman (1978) frequency values for a turn amount to 0.62×10^{-4} for wild-type vimentin, 0.15×10^{-4} for the G/V substitution, and to 0.50×10^{-4} for the R/E substitution; the cut-off value is 0.5×10^{-4}.) We also made an internal deletion extending from T-444 to V-452 (Fig. 1), to remove the entire β-site. The mutagenised constructs, in parallel to wild-type vimentin constructs, were cloned into a bacterial expression vector and expressed in *E. coli* (for details see Materials and Methods). Fig. 2a shows the bacterially synthesized recombinant vimentin, which (by gel scanning) amounted to approximately 14% of the total *E. coli* protein.

To isolate the vimentin tail mutants and the wild-type vimentin, we took advantage of the fact that the bacterially expressed proteins were segregated into inclusion bodies. Thus, the insoluble material was harvested by centrifugation of bacterial lysates and extracted with 1% Triton X-100 and 1 M urea. This treatment removed most of the contaminating proteins and yielded enriched fractions (Fig. 2b) from which we could further purify vimentin using ion-exchange chromatography (Fig. 2c) (for details see Materials and Methods).

Solubility properties and aggregation state of wild-type and mutant vimentin

To examine the properties of the vimentin tail mutants, we first studied their solubility as a function of ionic strength.

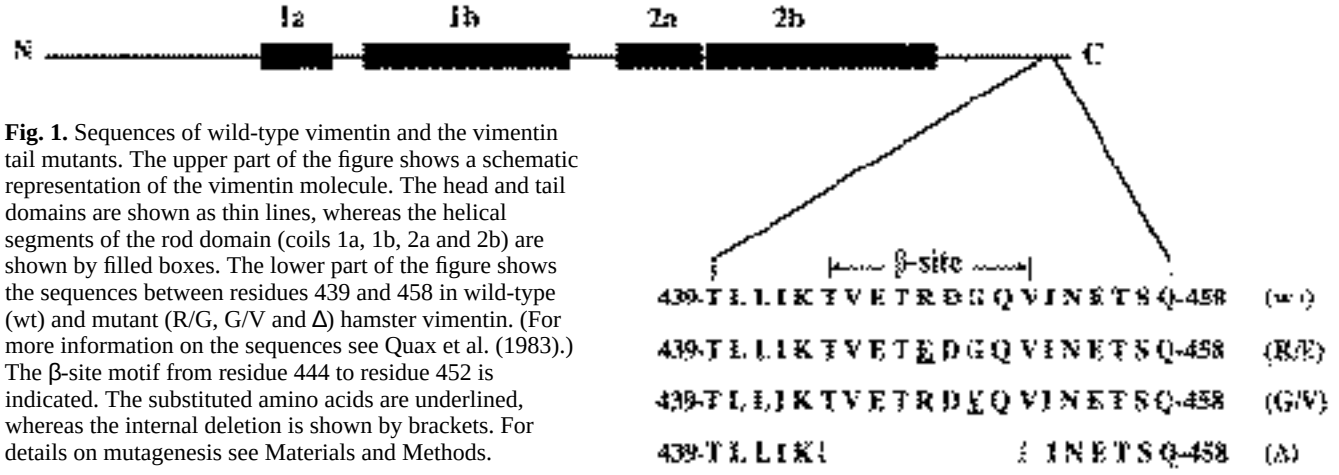

Fig. 1. Sequences of wild-type vimentin and the vimentin tail mutants. The upper part of the figure shows a schematic representation of the vimentin molecule. The head and tail domains are shown as thin lines, whereas the helical segments of the rod domain (coils 1a, 1b, 2a and 2b) are shown by filled boxes. The lower part of the figure shows the sequences between residues 439 and 458 in wild-type (wt) and mutant (R/G, G/V and Δ) hamster vimentin. (For more information on the sequences see Quax et al. (1983).) The β-site motif from residue 444 to residue 452 is indicated. The substituted amino acids are underlined, whereas the internal deletion is shown by brackets. For details on mutagenesis see Materials and Methods.

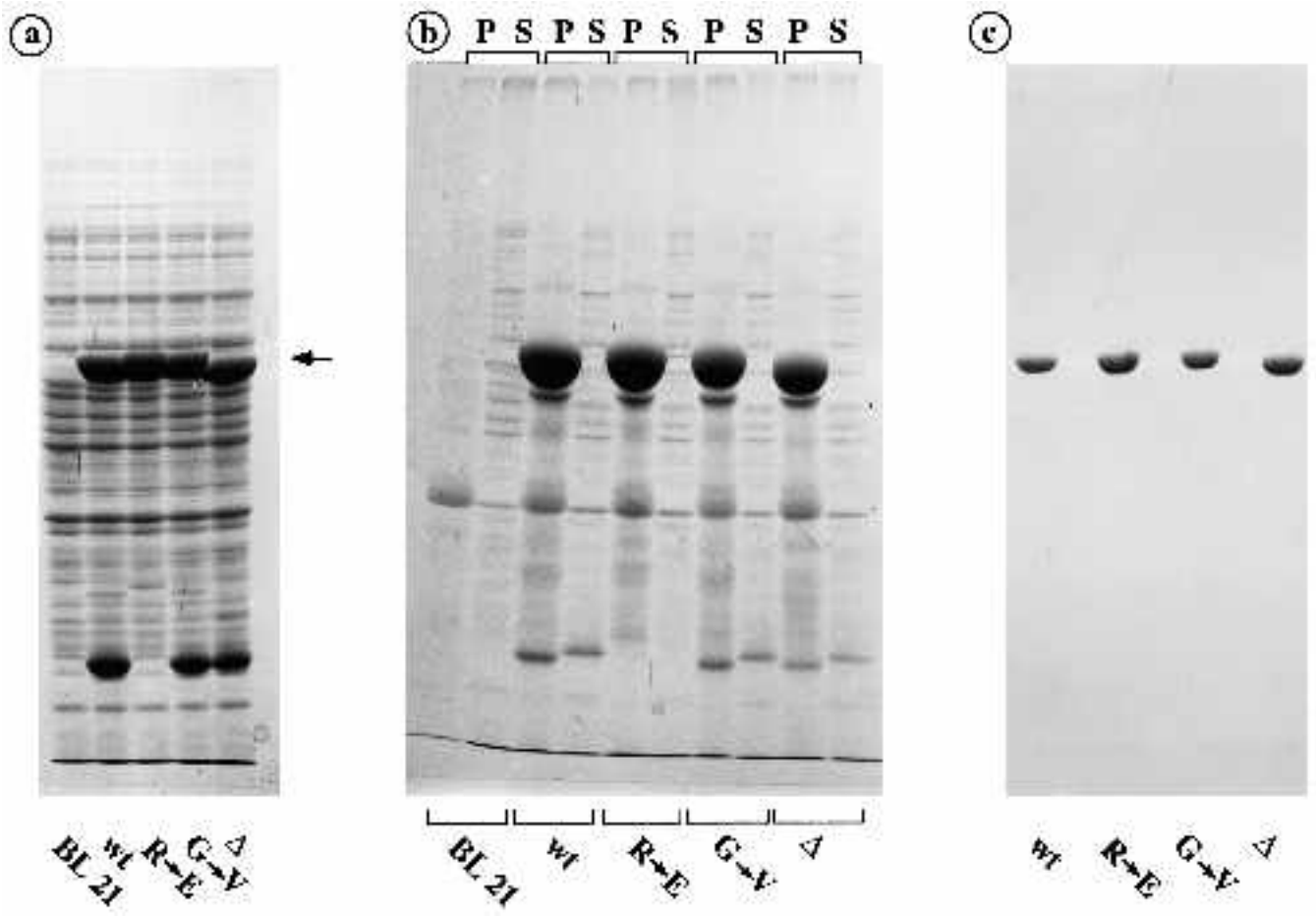

Fig. 2. Expression of vimentin tail mutants in *E. coli*, and protein purification. (a) Lysates from bacteria expressing the wild-type vimentin (wt) and the three tail mutants (as indicated) were analysed by SDS-PAGE, in parallel with a lysate of untransformed bacteria (BL 21). The arrow shows the position of vimentin. (b) Material from the lysates shown in (a) was centrifuged at low speed, the pellet extracted with 1% Triton X-100, and the detergent-insoluble residue re-extracted with 1% Triton X-100 and 1 M urea. The solubilized material (S) and the insoluble fraction after the second extraction (P) were electrophoresed in parallel and stained with Coomassie blue. Note that all vimentin forms are quantitatively recovered in the detergent/urea-insoluble fraction. (c) SDS-PAGE profile of the purified proteins (for details on the purification see Materials and Methods).

Monitoring the solution behavior of mutated proteins provides a useful guide for distinguishing assembly-defective from grossly misfolding subunits (for a relevant point see Moir et al., 1991). When the mutants and the wild-type vimentin were reconstituted in low salt buffer and ultracentrifuged, they remained largely soluble and partitioned

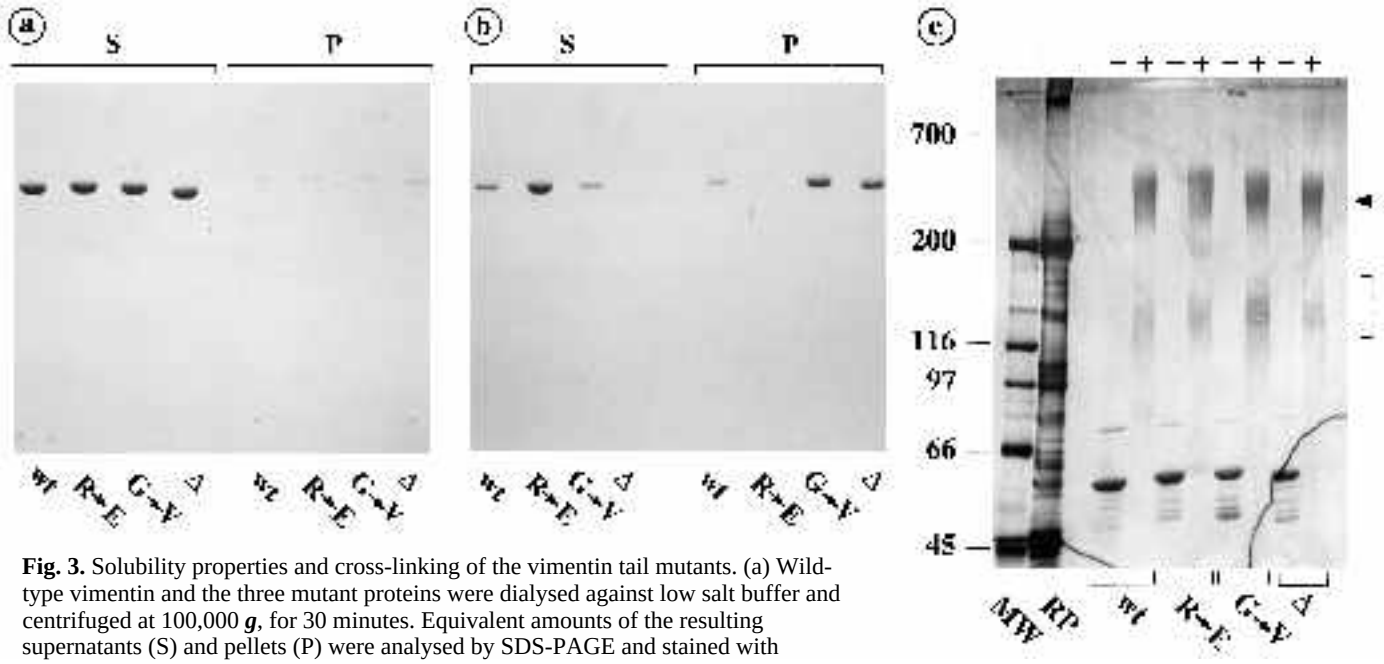

Fig. 3. Solubility properties and cross-linking of the vimentin tail mutants. (a) Wild-type vimentin and the three mutant proteins were dialysed against low salt buffer and centrifuged at 100,000 ***g***, for 30 minutes. Equivalent amounts of the resulting supernatants (S) and pellets (P) were analysed by SDS-PAGE and stained with Coomassie blue. (b) The same as in (a) with preparations dialysed against isotonic buffer and spun at 12,000 ***g*** for 5 minutes. (c) Cross-linking of the same preparations in 10 mM triethanolamine, pH 8.0, and analysis of the reaction products by SDS-PAGE in 5% to 10% acrylamide gradient gels. (+) and (−) indicate presence or absence of the cross-linker EGS. The cross-linked products corresponding to the molecular mass of a vimentin tetramer are indicated by an arrowhead. The broad bands included in brackets represent dimers. Numbers on the left indicate molecular masses in kDa, derived from the Bio-Rad molecular mass standards (MW) and from an extract of rabbit psoas muscle (RP). The 700 kDa marker corresponds to the protein nebulin (found in the muscle extract) and the 200 kDa marker corresponds to the myosin heavy chain.

with the supernatant fraction (Fig. 3a). However, when the same preparations were reconstituted into isotonic buffer and centrifuged at low speed (12,000 ***g*** for 5 minutes), we noticed that G/V and the deletion mutant formed readily pelletable aggregates (Fig. 3b). In contrast, wild-type vimentin and the R/E mutant did not significantly pellet under the same conditions (Fig. 3b). These experiments suggested that, whereas all three mutant proteins behave similarly to wild-type subunits in low salt, G/V and the deletion mutants aggregate under conditions favouring IF assembly.

To further assess the ability of the mutants to oligomerize at low ionic strength, we performed cross-linking experiments. Fig. 3c illustrates the finding that the wild-type vimentin as well as the mutant proteins formed dimers, tetramers and higher oligomers. As previously shown (Geisler and Weber, 1982), the tetramers represented the most populated (but not the sole) species under these conditions. Similar results were obtained when the proteins were cross-linked in low salt buffer containing 4 M urea (M. Brunkener and S. D. Georgatos, unpublished observations).

To examine whether the tail mutations affect the overall conformation of vimentin, we compared the G/V mutant and the deletion mutant with wild-type vimentin using circular dichroism (CD) spectroscopy. In media containing 5 mM Na_3PO_4, pH 8.0, the spectra of the mutant proteins were similar to the spectrum of wild-type vimentin (A. Politou and S. D. Georgatos, unpublished results). Thus, these two mutants did not show a change in the secondary structure in comparison to the wild-type protein.

In vitro assembly properties of the vimentin tail mutants

To investigate the filament-forming ability of the tail mutants, we performed in vitro assembly experiments and examined the structures formed by electron microscopy. Upon dialysis from 8 M urea to isotonic salt, wild-type vimentin polymerized into long, smooth and unbranched IFs (Fig. 4a). Under the same conditions, the R/E mutant polymerized into long filaments (Fig. 4b). The diameter of these filaments was largely normal, except that they appeared to ‘unravel’ at certain segments more frequently than wild-type vimentin (Fig. 4b). The G/V mutant assembled into irregular fibrils that possessed a rough surface (Fig. 4e). The fibrils were laterally aggregated and extensively anastomosed, forming a variety of ‘honeycomb’ structures (Fig. 4c). Finally, the deletion mutant assembled very aberrantly and, under comparable conditions, yielded large aggregates (Fig. 4d) that appeared to consist of thick

Fig. 4. Assembly of vimentin tail mutants in isotonic media using the standard dialysis protocol. Negatively stained samples of wild-type vimentin (a), the R/E mutant (b), the G/V mutant (c) and the deletion mutant (d) are shown in the first four panels. (e) and (f) show higher magnifications of the area included between the arrows in (c) and (d), respectively. Note the abberant morphology and the aggregation of the filaments formed by G/V and the deletion mutant. Arrows in (b) point to segments of the filaments showing a ribbon-like structure. All preparations have been reconstituted by dialysis against isotonic buffer, for 3 hours at room temperature. Bars, 100 nm.

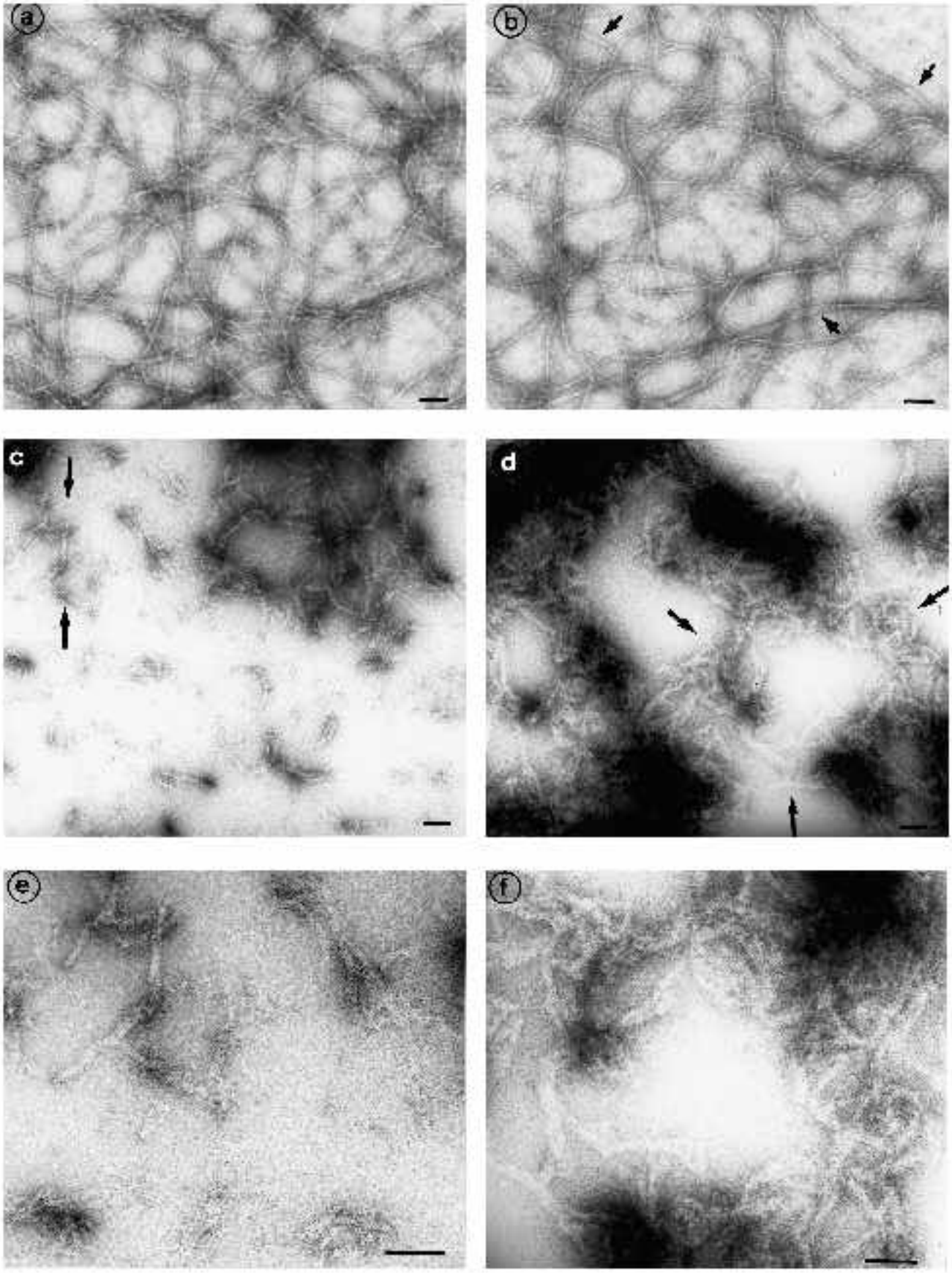

Fig. 4

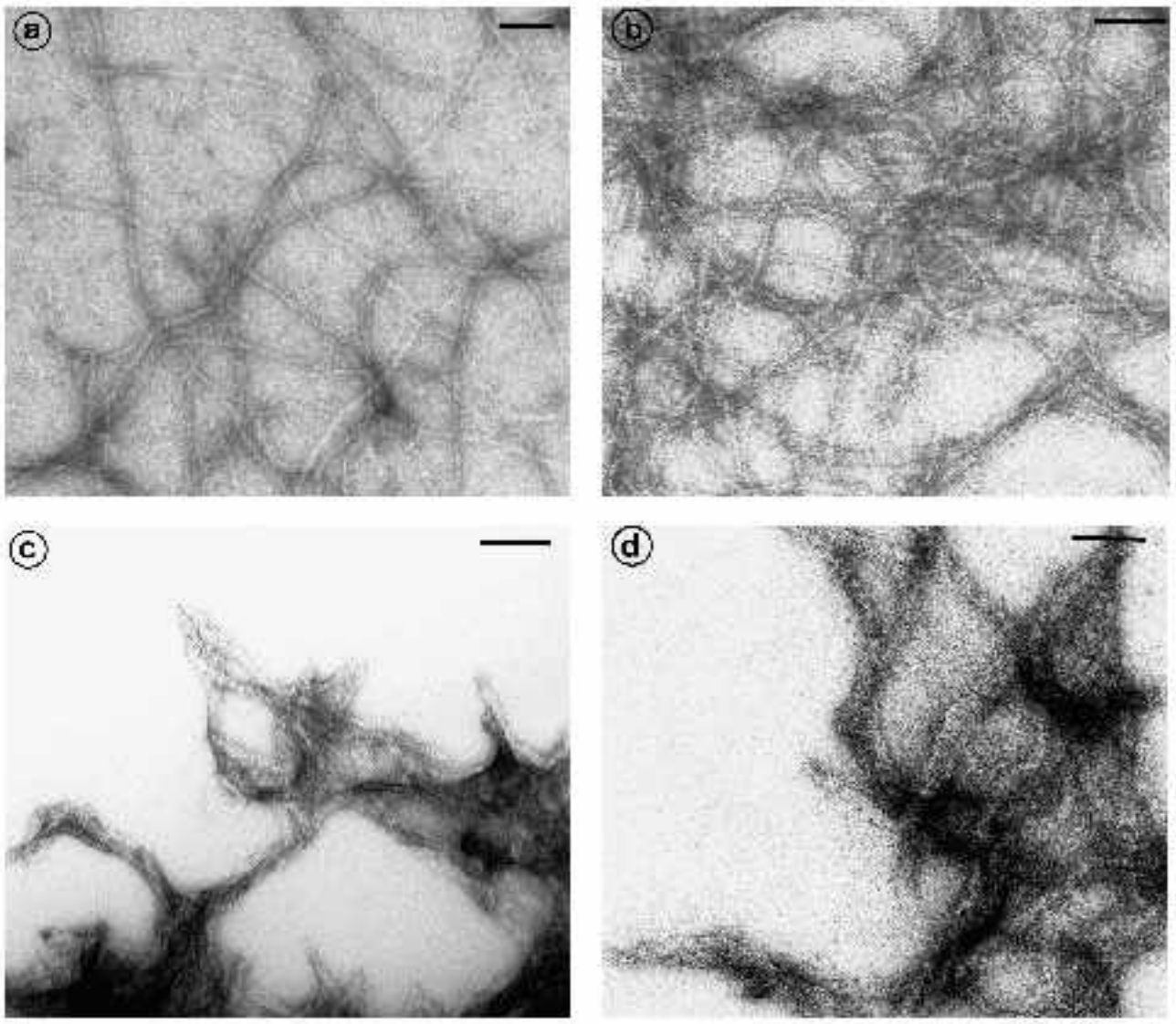

Fig. 5. Assembly of vimentin tail mutants in isotonic media using a stepwise dialysis protocol. Negatively stained samples of the wild-type vimentin (a), the R/E mutant (b), the G/V mutant (c), and the deletion mutant (d) are shown. The preparations have been sequentially dialysed against low salt (3 hours at 4°C), isotonic buffer (overnight, at 4°C), and isotonic buffer (2 hours at 37°C). Note the lateral aggregation of the filaments formed by the G/V mutant, the beading of the fibrils formed by the deletion mutant, and the nearly normal appearance of the filaments assembled from the R/E mutant. Bars, 100 nm.

(20-25 nm) fibers of a beaded or 'granular' texture (see Fig. 4f and below). Thin-sectioning and transmission electron microscopy of the aggregates formed by G/V and the deletion mutant confirmed the fibrillar nature of these assemblies (not shown).

Assembly in the presence of 10 mM $CaCl_2$ did not alter the ultrastructure of the filaments assembled from mutant vimentin (M. Brunkener and S. D. Georgatos, unpublished results). Thus, the hamster tail mutant vimentins seemed to differ from tail-less *Xenopus laevis* vimentin, which forms very thick paracrystalline structures in 5-20 mM $CaCl_2$ (Eckelt et al., 1992).

To examine further whether the aggregation of the mutant subunits was the result of a 'too fast' self-association reaction (see Stewart, 1993), we performed experiments in which the vimentin mutants were assembled in a stepwise manner. The preparations were first dialysed against low salt (to renature the urea-solubilized subunits without promoting polymerization), then against isotonic salt at 4°C (to slowly initiate the assembly of filaments), and finally against isotonic salt at 37°C (to effect complete polymerization). As shown in Fig. 5b, the R/E mutant yielded nearly normal filaments. However, the G/V mutant produced aggregates consisting of small bundles of laterally associated filaments (Fig. 5c), whereas the deletion mutant polymerized into thick fibrils that exhibited a quasi-regular beading with a periodicity of ~20.5 nm (Fig. 5d). Thus, the aberrant assembly of the latter two mutants could not be rectified by simple modifications in the assembly protocol, which are expected to slow down IF polymerization.

To find out whether the assembly-defective mutants

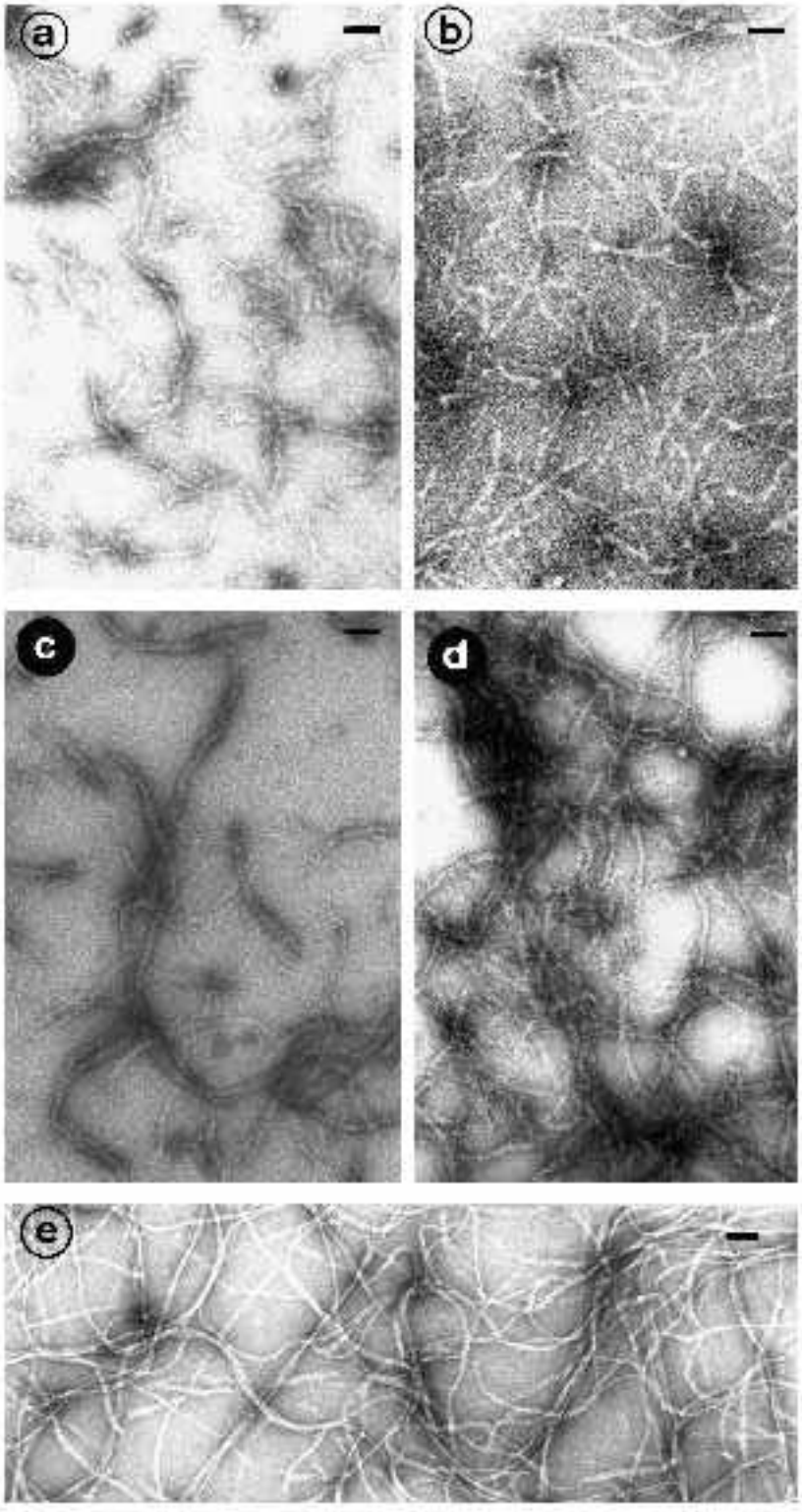

Fig. 6. Co-assembly of wild-type vimentin and vimentin tail mutants. Each of the two assembly-defective mutants (a, b, G/V mutant; c, d, deletion mutant) was mixed with wild-type vimentin in ratios of 9:1 (a, c) or 1:1 (b, d) in 8 M urea buffer and then dialysed as specified for Fig. 4. In (e), an equimolar mixture of the wild-type vimentin and the deletion mutant was dialysed in a stepwise fashion, as described for Fig. 5. Note the lower degree of aggregation and the persistence of the mutant filament phenotype in (a-d). Also note the nearly normal appearance of the filaments in (e). Bars, 100 nm.

could be 'rescued' by wild-type subunits, we performed mixing experiments. As shown in Fig. 6a-d, when the two assembly-defective mutants were co-assembled with wild-type vimentin in ratios varying from 9:1 to 1:1 the formation of aggregates was substantially suppressed. However, the morphology of the filaments remained abnormal. The wild-type and the mutant subunits did not assemble into separate polymers because all of the filamentous forms that we detected appeared identical and there was no indication of 'islands' of normal-looking IFs anywhere in the fields. Thus, incorporation of substoichiometric amounts of wild-type protein into the (hybrid) filaments can apparently reduce the aggregation of the filaments without totally rectifying their abnormal surface morphology. Interestingly,

Fig. 7. Assembly of vimentin tail mutants at low salt media. Negatively stained preparations of wild-type vimentin (a), the G/V mutant (b) and the deletion mutant (c). These samples have been dialysed against low salt buffer, for 3 hours at room temperature. Note the presence of short, rod-like particles in all three cases. Bars, 100 nm.

when the stepwise assembly protocol was used (see above), the 1:1 mixture of wild-type vimentin and the deletion mutant yielded nearly normal filaments, exhibiting only a slight variation in diameter (Fig. 6e). This could mean that the co-assembly of mutant and wild-type subunits is more efficient when polymerization is induced in a stepwise manner.

Finally, to differentiate between assembly defects at the level of lower oligomers from aberrant subunit-subunit interactions at the level of filaments, we examined by electron microscopy the two assembly-defective mutants after dialysis against low ionic strength buffer. As shown in Fig. 7b and c, G/V and the deletion mutant formed 5-7 nm rod-like fibrils with an irregular surface morphology (Fig. 7b and c). These particles were similar to the structures formed by wild-type vimentin (Fig. 7a) and may correspond to protofibrils or other IF assembly intermediates (for pertinent information on the ultrastructure of lower aggregates of vimentin see Ip et al., 1985; for models on the early assembly intermediates of IFs see Aebi et al., 1983). Apparently, the structures formed after dialysis against 5 mM Tris-HCl at pH 7.4 are different from the regular vimentin protofilaments (tetramers), which represent the predominant species after cross-linking at 10 mM triethanolamine at pH 8.0 (see Fig. 3c). This is probably due to the fact that the alkaline pH used in the cross-linking experiments suppresses the formation of higher vimentin oligomers.

DISCUSSION

In this study, we have examined the in vitro properties of vimentin mutagenized in the region of the β-site, a conserved motif previously identified in the COOH-terminal region of vimentin, desmin and peripherin (Kouklis et al., 1991). We have found that vimentin harbouring a point mutation at G-450, or lacking the entire β-site (T-444 to V-452), polymerizes aberrantly and yields laterally aggregated filaments. In contrast, a point mutation in R-448 produces a very mild phenotype and forms nearly normal IFs. Since all mutants tetramerize and form similar oligomers under low salt conditions, the simplest interpretation would be that G/V and the deletion mutant assemble appropriately up to the level of protofilaments and protofibrils but are compromised in their ability to participate in a more complex series of molecular interactions that lead to smooth and unbranched IFs.

The filaments produced by the G/V mutant are not (as such) thicker than normal IFs but show a strong tendency to anastomose and laterally aggregate. Thus, a single point mutation at G-450, although drastically affecting the surface properties of IFs, does not seem to disturb the lateral growth of individual filaments. However, when the whole β-site is excised, the filaments are both aggregated and thicker, suggesting that protofilament-protofilament interactions within the same filament have been affected. The 'stickiness' of the mutant IFs (which finally leads to lateral aggregation) may be due to the fact that some 'acceptor sites' along the surface lattice of IFs remain unsaturated as a result of protofilament misalignment. On the other hand, the increase of the filament diameter probably reflects a more severe pertubation in which the entire helical arrangement of the subunits along the filament axis is faulty. Interestingly, these defects cannot be rectified by simple changes in the ionic milieu, as has been the case with tail-truncated desmin (Kaufman et al., 1985), or with cytokeratins mutagenized in the conserved coil 2b motif (Hatzfeld and Weber, 1991). From this it can be concluded that the misalignment of the mutant protofilaments involves more than a mere disturbance of the ionic interactions between adjacent subunits. However, as shown above, the aggregation of mutant vimentin is effectively suppressed by 'diluting' the mutant with wild-type subunits.

The data presented here rule out the possibility that the aberrant behavior of the tail mutants is due to a global misfolding of the polypeptide chain. Moreover, the severity of the aberrant filament phenotypes matches the expected degree of pertubation of the (predicted) β-turn motif (TRDG) that is included in the β-site. Thus, by secondary structure prediction one anticipates that the potential for a β-turn in this region would decrease in the order: wild type > R/E > G/V > deletion mutant, which reflects the degree of abnormality in the filament phenotypes that we have observed. This is in line with the idea that the introduced mutations affected the regional structure of the β-site.

As mentioned in the Introduction, the role of the tail domain in IF assembly is controversial. While most of the published studies using tail-less and tail-truncated mutants suggest an important role for this domain in IF assembly, filamentous assemblies can apparently be obtained from certain tail-less IF proteins. However, more careful analysis reveals that the assembly characteristics and the physicochemical properties of tail-less proteins differ from those of the wild-type proteins. For example, tail-less cytokeratins need a higher salt concentration to assemble into regular IFs (Hatzfeld and Weber, 1990), whereas tail-less vimentin polymerizes more efficiently and aggregates to a higher extent than normal vimentin in the presence of Ca^{2+} (Eckelt et al., 1992). Thus, the tail domain, although not essential as such for the polymerization of IF proteins, appears to be involved in regulatory or stabilizing interactions that are important for normal filament structure (Hatzfeld and Weber, 1990; Wilson et al., 1992). More specifically, the COOH-terminal region of IF proteins (or a motif therein) may interact with 'acceptor sites' located in other parts of the IF molecule and these interactions may influence the lateral packing and the surface properties of IFs.

Whereas the radical deletion of the tail domain would not allow identification of those parts of the domain that are involved in subunit-subunit interactions, point mutations and limited internal deletions in this region may facilitate the characterization of sites involved in the self-association reactions. For example, the finding that mutations in the β-site interfere with vimentin assembly in vitro indicates that this motif probably represents such a self-association site. However, since mutation analysis alone does not suffice to explain the role of the tail domain in filament assembly, it is useful to consider here some previous experiments. We have recently shown that when wild-type vimentin is assembled in the presence of a synthetic peptide that

includes the β-site, the filaments grow thicker and laterally aggregate into bundles (Kouklis et al., 1991). Milder, but yet noticable effects were observed when desmin subunits were assembled in the presence of another peptide that includes the same motif (Birkenberger and Ip, 1990). These experiments suggest that β-site derivatives may compete with wild-type vimentin molecules for binding to one or more acceptor sites. One such site (ε) has already been identified and mapped in the area between residues 364 and 416 of vimentin (Kouklis et al., 1991). There are some indications that the stretch between residues 410 and 416, which has been removed in the tail-less vimentin constructs (Eckelt et al., 1992), may be part of the ε-site (P. D. Kouklis, T. Papamarcaki and S. D. Georgatos, unpublished observations). From these data it would appear that when both the ε and the β-sites are excised, the filaments can grow normally, whereas when one of the two sites is 'neutralized' (by competition with synthetic peptides or by mutation), the filaments show aberrant assembly behavior. It remains to be further examined whether the filaments assembled from tail-less vimentin and β-site-mutagenized vimentin possess the same number of polypeptide chains per filament cross-section and whether they are as stable and as modulatable by phosphorylation as bona fide IFs.

This work is dedicated to Adamantia and Stavros Politis. We extend our thanks to Anastasia Politou for recording the CD spectra of vimentin, and to Fotini Gounari for help in DNA sequencing. P.D. Kouklis was supported by an EMBL post-doctoral fellowship.

REFERENCES

Aebi, U., Fowler, W. E., Rew, P. and Sun, T. T. (1983). The fibrillar substructure of keratin filaments unraveled. *J. Cell Biol.* **97**, 1131-1143.

Albers, K. and Fuchs, E.B. (1987). The expression of mutant epidermal keratin cDNAs transfected in simple epithelial and squamus cell carcinoma lines. *J. Cell Biol.* **105**, 791-806.

Albers, K. and Fuchs, E.B. (1989). Expression of mutant keratin cDNAs in epithelial cells reveals possible mechanisms for initiation and assembly of intermediate filaments. *J. Cell Biol.* **108**, 1477-1493.

Bader, B.L., Magin, T.M., Freudenmann, M., Stumpp, S. and Franke, W. W. (1991). Intermediate filaments formed de novo from tail-less cytokeratin in the cytoplasm and in the nucleus. *J. Cell Biol.* **115**, 1293-1307.

Birkenberger, L. and Ip, W. (1990). Properties of the desmin tail domain: studies using synthetic peptides and antipeptide antibodies. *J. Cell Biol*. **111**, 2063-2075.

Bujard, H., Gentz, R., Lanzer, M., Stüber, D., Müller, M., Ibrahimi, I., Häuptle, M. T. and Dobberstein, B. (1987). A T5 promotor-based transcription-translation system for the analysis of proteins in vitro and in vivo. *Meth. Enzymol.* **155**, 416-433.

Chou, P. V. and Fasman, G. D. (1978). Prediction of the secondary structure of proteins from their amino acid sequence. *Adv. Enzymol.* **47**, 45-148.

Eckelt, A., Herrmann, H. and Franke, W. W. (1992). Assembly of a tail-less mutant of the intermediate filament protein, vimentin, in vitro and in vivo. *Eur. J. Cell Biol.* **58**, 319-330.

Geisler, N. Schünemann, J. and Weber, K. (1992). Chemical cross-linking indicates a staggered and antiparallel protofilament of desmin intermediate filaments and characterizes one higher-level complex between protofilaments. *Eur. J. Biochem.* **206**, 841-852.

Geisler, N. and Weber, K. (1982). The amino acid sequence of chicken muscle desmin provides a common structural model for intermediate filaments. *EMBO J.* **1**, 1649-1656.

Hatzfeld, M., Dodemont, H. Plessmann, U. and Weber, K. (1992). Truncation of recombinant vimentin by ompT. Identification of a short motif in the head domain necessary for assembly of type III intermediate filament proteins. *FEBS Lett.* **302**, 239-242.

Hatzfeld, M. and Weber, K. (1990). Tail-less keratins assemble into intermediate filaments in vitro. *J. Cell Sci.* **97**, 317-324.

Hatzfeld, M. and Weber, K. (1991). Modulation of keratin intermediate filament assembly by single amino acid exchanges in the consensus sequence at the C-terminal end of the rod domain. *J. Cell Sci.* **99**, 351-362.

Herrmann, H., Hofmann, I. and Franke, W. W. (1992). Identification of a nonapeptide motif in the vimentin head domain involved in intermediate filament assembly. *J. Mol. Biol.* **223**, 637-650.

Hofmann, I. and Herrmann, H. (1992). Interference in vimentin assembly in vitro by synthetic peptides derived from the vimentin head domain. *J. Cell Sci.* **101**, 687-700.

Ip, W., Heuser, J. E., Pang, Y-Y. S., Hartzer, M. K. and Robson, R. M. (1985). Subunit structure of desmin and vimentin protofilaments and how they assemble into intermediate filaments. *Ann. NY Acad. Sci.* **455**, 185-199.

Kaufmann, E., Weber, K. and Geisler, N. (1985). Intermediate filament forming ability of desmin derivatives lacking either the amino-terminal 67 or the carboxy-terminal 27 residues. *J. Mol. Biol.* **185**, 733-742.

Kouklis, P.D., Papamarcaki, T., Merdes, A. and Georgatos, S.D. (1991). A potential role for the COOH-terminal domain in the lateral packing of type III intermediate filaments. *J. Cell Biol.* **114**, 773-786.

Kouklis, P. D., Traub, P. and Georgatos, S. D. (1992). Involvement of the consensus sequence motif at coil 2b in the assembly and stability of vimentin filaments. *J. Cell Sci.* **102**, 31-41.

Kunkel, T. A., Roberts, J. D. and Zakour, R. A. (1987). Rapid and efficient site-specific mutagenesis without phenotypic selection. *Meth. Enzymol.* **154**, 367-382.

Laemmli, U. K. (1970). Cleavage of structural proteins during the assembly of the head of bacteriophage T4. *Nature* **227**, 680-685.

Lu, X. and Lane, E. B. (1990). Retrovirus-mediated transgenic keratin expression in cultured fibroblasts:Specific domain functions in keratin stabilisation and filament formation. *Cell* **62**, 681-696.

Moir, R. D., Donaldson, A. D. and Stewart, M. (1991). Expression in Escherichia coli of human lamins A and C: influence of head and tail domains on assembly properties and paracrystal formation. *J. Cell Sci*. **99**, 363-372.

Nakamura, Y., Takeda, M., Aimoto, S., Hariguchi, S., Kitajima, S. and Nishimura, T. (1993). Acceleration of bovine neurofilament L assembly by deprivation of acidic tail domain. *Eur. J. Biochem.* **212**, 565-571.

Quax, W., Egberts, W. V., Hendriks, W., Quax-Jeuken, Y. and Bloemendal, H. (1983). The structure of the vimentin gene. *Cell* **35**, 215-223.

Quinlan, R. A., Moir, R. D. and Stewart, M. (1989). Expression in Echerichia coli of fragments of glial fibrillary acidic protein: characterization, assembly properties and paracrystal formation. *J. Cell Sci.* **93**, 71-83.

Raats, J. M. H., Pieper, F. R., Vree Egberts, W. T. M., Verrijp, K. N., Ramaekers, F. C. S. and Bloemendal, H. (1990). Assembly of amino-terminally deleted desmin in vimentin-free cells. *J. Cell Biol.* **111**, 1971-1985.

Raats, J. M. H., Henderik, J. B. J., Verdijk, M., van Oort, F. L. G., Gerards, W. L. H., Ramaeckers, F. S. C. and Bloemendal, H. (1991). Assembly of carboxy-terminally deleted desmin in vimentin-free cells. *Eur. J. Cell Biol.* **56**, 84-103.

Shoeman, R. L., Mothes, E., Kesselmeier, C. and Traub, P. (1990). Intermediate filament assembly and stability in vitro: Effect and implications of the removal of head and tail domains of vimentin by the human immunodeficiency virus type I protease. *Cell Biol. Int. Rep.* **14**, 583-594.

Stewart, M. (1993). Intermediate filament structure and assembly. *Curr. Opin. Cell Biol.* **5**, 3-11.

Traub, P. and Vorgias, C. E. (1983). Involvement of the N-terminal polypeptide of vimentin in the formation of intermediate filaments. *J. Cell Sci.* **63**, 43-67.

Wilson, A. K., Coulombe, P. A. and Fuchs, E. (1992). The roles of K5 and K14 head, tail and R/K L L E G E domains in keratin filament assembly in vitro. *J. Cell Biol.* **119**, 401-414.

Wong, P. C. and Cleveland, D. W. (1990). Characterization of dominant and recessive assembly defective mutations in mouse neurofilament NF-M. *J. Cell Biol.* **111**, 1987-2004.